YTUP

Journal of Thermal Engineering

https://jten.yildiz.edu.tr/

https://doi.org/10.47481/jten.0045

RESEARCH ARTICLE

Computational fluid dynamics study (CFD) of cooling systems heat transfer fluids (HTFS) for electrical cabins

Abderrahmane Elmeriah[1], Abdelfatah Marni Sandid[2,*], Seddik Taieb[3], Driss Nehari[4], Faiza Chouli[5]

[1]Department of Mechanical Engineering, Faculty of Sciences and Technology, University of Mustapha Stambouli Mascara, BP 305 Route de Mamounia, Mascara, 29000, Algeria
[2]Center of Research in Mechanics (CRM), BP N73B, Freres Ferrad, Ain El Bey, Constantine, 25021, Algeria
[3]Laboratory of Quantum Physics and Mathematical Modeling of the Material (LPQ3M), University of Mascara, Mascara, 29000, Algeria
[4]Department of Mechanical Engineering, Route Sidi Bel Abbes, BP 284, University of Ain Temouchent, Ain Temouchent, 46000, Algeria
[5]LMAE Laboratory, Department of Process Engineering, Faculty of Sciences and Technology, University of Mustapha Stambouli Mascara, BP 305 Route de Mamounia, Mascara, 29000, Algeria

Abstract

This numerical study examines heat transfer phenomena, with particular focus on evaluating the cooling performance of embedded cavity technologies for electrical and electronic enclosure applications. The thermo-fluidic characteristics of laminar flow within a confined cavity bounded by isothermal heat sources were analyzed by experimentally measuring thermophysical of premixed binary fluids comprising water and ethylene glycol (EG) at concentrations ranging from 25% to 100%. The Navier-Stokes equations governing this steady-state open system are solved numerically using the finite volume method implemented in the commercial computational fluid dynamics (CFD) software Ansys Fluent v17. This computational approach enables precise determination of convective heat transfer characteristics during the cooling process. Key results are presented in terms of the mixture's surface-averaged Nusselt number, total Nusselt number, and cooling efficiency within the cavity at various ethylene glycol concentrations (25-100%). Comparative analysis reveals that ethylene glycol coolant exhibits significantly superior cooling performance compared with pure water. This enhancement is demonstrated by progressive increases in both the total Nusselt number (from 11.5 to 14.8, 16.5, 21.8, and 35.9) and in cooling efficiency (from 87.4% to 92%, 95.2%, 97%, and 98.3%), corresponding to ethylene glycol concentrations of 25%, 50%, 75%, and 100%, respectively. Furthermore, enhanced thermo-fluidic behavior is consistently observed with increasing ethylene glycol content.

Keywords: Forced convection, computational fluid dynamics (CFD), electrical cabins, ethylene glycol coolant

Cite this article as: Elmeriah, A., Marni Sandid, A., Taieb, S., Nehari, D., & Chouli, F. (2026). Computational fluid dynamics study (CFD) of cooling systems heat transfer fluids (HTFS) for electrical cabins. Journal of Thermal Engineering, 12(4), 1480–1492. https://doi.org/10.47481/jten.0045

1. Introduction

Modern technological applications in the industrial, automotive, and medical sectors have achieved significant efficiency gains through advancements in thermal management systems. These systems play a critical role in maintaining energy cycles for electronic, electrical, and thermal processing applications that are creating a growing demand for innovative cooling solutions. This is particularly critical for thermal processes requiring enhanced heat-transfer mechanisms, including conduction and convection. Enhancing heat transfer techniques has emerged as a compelling research area with scientists exploring diverse materials to optimize thermal exchange processes [1] [2]. Heat transfer fluids (HTFs) play a pivotal role in industrial and technological applications, serving dual functions as thermal media that absorb or dissipate heat and as lubricants in mechanical systems [3]. In this context, previous research [4-8] has extensively studied natural convection heat

*Corresponding Author
E-mail Adress: abdelfatahsandid@hotmail.com

Submitted: 26 February 2025; **Accepted:** 19 August 2025

This paper was recommended for publication in revised form by Editor-in-Chief Ahmet Selim Dalkılıç

Published by Yıldız Technical University, İstanbul, Türkiye

transfer in two-dimensional (2D) enclosed containers, by the way of numerical simulations using the finite difference method (FDM) for steady laminar flow of Newtonian fluids demonstrated that increasing Rayleigh numbers significantly enhances both the Nusselt number and natural convection intensity. Within the same framework, a similar studies [9] employing the finite volume method (FVM) analyzed water-filled square cavities containing embedded circular bodies between differentially heated walls. These investigations revealed that circular structures enhance the thermo-hydraulic properties of water, particularly with respect to entropy generation and convective heat transfer coefficients. Recent work has focused on geometrically complex internal heat sources in Newtonian fluid-filled containers to analyze the thermo-fluidic behavior around hot obstacles. Practically, multiple experimental and numerical studies [10-13] consistently show that elevated Rayleigh numbers substantially improve the average of heat transfer coefficients, which making the convection heat transfer interchange increasingly dominant over conduction. Among the geometrical parameters studied, square containers remain a primary focus in this field, with some modifications conducted according to recent investigations [14] that examine wavy sidewall effects on incompressible fluid heat circulation. These studies type has demonstrated that wall undulation is significantly influences both flow patterns and heat transfer rates, though research in porous media [15] that indicates for an excessive undulation can reduce the average of heat transfer performance. A numerical study [16] investigates the natural convection cooling of a bottom-mounted heat source in a cold-walled cavity under two thermal conditions (constant heat flux or temperature). The key parameters include Rayleigh number ($10^3 \leq Ra \leq 10^6$), source length($0.1 \leq SL \leq 1.0$),lateral position(D)and Prandtl number($0.71 \leq Pr \leq 10^2$).Here, the results reveal enhanced heat transfer (quantified by the Nusselt number) with increasing Ra and SL, except at high Ra in constant-temperature cases. Optimal cooling occurs for SL = 0.1 and D = 0 (left-aligned source), with heat transfer improving significantly up to Pr = 5 before stabilizing for Pr > 50.

In their work, the authors of [17] explored whether adding nanoparticles to a base fluid could improve cooling by natural convection in a cavity with a heater located at the bottom. Their calculations were performed using a finite-volume model together with the SIMPLE procedure. They analyze how the Rayleigh number, heat source geometry and location, nanoparticle type (Al_2O_3, CuO, etc.), and volume fraction (0-5%) affect thermal performance. The simulations showed that nanoparticle addition contributes to more effective heat dissipation, especially in low-convection regimes ($Ra < 10^4$). At the same time, the thermal response of the enclosure depended considerably on the shape and location of the heat source. For the same technic, a numerical study has been performed [18] to analyze the natural convection in a CNT-water Nano-fluid filled inside the square enclosure under a magnetic field and source heat throughout two thin fins. In this computational fluid dynamics (CFD) analysis using the control volume method, several examinations were conducted to determine how fin geometry (position, length, and spacing), nanoparticle concentration (φ), and Rayleigh (Ra) and Hartmann (Ha) numbers affect heat transfer, with results showing that heat transfer increases with higher Ra, φ, and fin length but decreases with increasing Ha. By the same numerical approach of a mixed convection in a square container, that containing copper-water Nano-fluid, featuring inlet/outlet ports and a bottom-mounted constant-flux heat source has been investigated [19]. Employing a finite volume method with the SIMPLE algorithm, they analyze the coupled effects of Reynolds ($50 \leq Re \leq 1000$) and Richardson ($0 \leq Ri \leq 10$) numbers along with nanoparticle volume fraction ($0 \leq \phi \leq 0.05$). The Patel (thermal conductivity) and Brinkman (viscosity) models characterize nanofluid properties. Results indicate that increasing ϕ enhances heat transfer, quantified by the Nusselt number, and reduces the bulk temperature, as visualized by streamlines and isotherms. The other numerical method using finite element method has been conducted [20] to examine the mixed convection in a rectangular enclosure with practical relevance to electronic cooling systems. The configuration features a sinusoidally heated right wall, a cooled left wall, and insulated horizontal surfaces, with flow entering at the bottom-right and exiting at the top-left. Using COMSOL Multiphysics (FEM), a CFD analysis has been carried out for the Richardson impact ($0 \leq Ri \leq 10$) and Reynolds ($50 \leq Re \leq 200$) numbers, along with heat source positioning (bottom-left/center/top-right) on thermal performance through Nusselt number, streamline and isotherm distributions.

The role of nanotechnology in pushing this field forward [21-25] is well reflected through nano-fluids (Cu/H2O, Al2O3/H2O, TiO3/H2O), which tend to promote stronger natural convection, a behavior largely tied to how well these mixtures conduct heat. Turning to square enclosures fitted with inlet/outlet openings (opened system), CFD-based investigations [26] [27] run through Fluent software looked at how factors like the enclosure width (W) and the placement of the ports (s) come into play. Their results showed that a suitable outlet position could enhance heat transfer while keeping pressure losses relatively low. Other work [28,29] focused on compressible heat-transfer fluids flowing through square and rectangular enclosures with opposing openings. As the Reynolds and Richardson numbers increased, the flow behavior changed progressively, and natural convection became more influential. COMSOL Multiphysics simulations were also carried out to study cavities fitted with baffles and multiple outlets. Such findings shed light on the extent to which both working conditions and enclosure geometry play a role in determining how effectively heat is removed. Building on these previous studies, the present work investigates cooling in a square cavity through a combined experimental and numerical approach. Ethylene glycol–water mixtures with concentrations ranging from 25% to 100% were first characterized experimentally, after which their forced-convection behavior in open laminar-flow configurations was examined numerically. This work provides new insights into binary fluid behavior while addressing practical cooling challenges in modern thermal applications.

2. Physical and mathematical description

2.1. Physical model

The two-dimensional (2D) physical model considered in this study is shown in Figure 1, where the linear dimensions of the square cavity along the x and y directions are denoted by L and H. The entrance of the fluid will be through an inlet side, which is located on the left vertical wall, extending from y = (H - Wi) to y = H. An outlet side has opposite position to the inlet port and fixed location of(2 + 0.5W)according to the special coordinate system(s)along the walls that started from x = 0 and y = H as clarified by the dashed lines in Figure 1. Here the widths of the inlet and outlet ports are identical (wi = wo = w). The inlet temperature of the fluid is Tin, where the four external walls of the cavity are conditioned at temperature Tw with Tw > Tin.

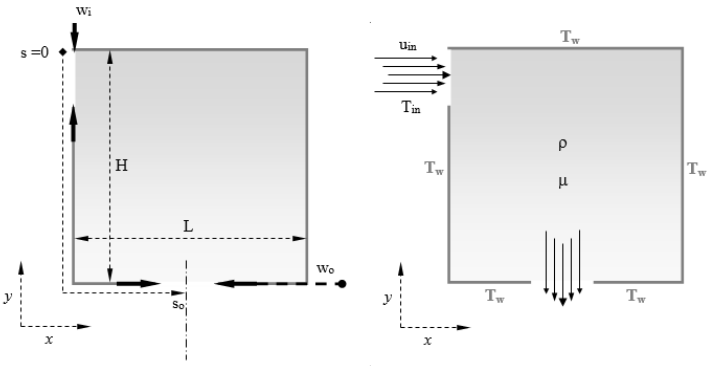

Figure 1. Dimensions of the physical model used [26]

2. 2. Mathematical and numerical methods

This study considers a steady flow field with constant properties. The variable dimensionless terms are written in the governing equations, where the cavity lengths, inlet fluid velocity and wall/fluid temperatures can be expressed by H, u_{in}, T_w and T_{in}, respectively. The dimensionless variables (denoted by capital letters) are defined as follows:

$$X = \frac{x}{H}, Y = \frac{y}{H}, U = \frac{u}{u_{in}}, V = \frac{v}{u_{in}}, P = \frac{p}{\rho u_{in}^2}, \theta = \frac{T - T_{in}}{T_w - T_{in}} \qquad (1)$$

The dimensionless parameters X, Y, U, V, P, and θ constitute normalized representations of fundamental physical variables in the flow system. The spatial coordinates are non-dimensionalized by dividing by the characteristic length scale H (X = x/H, Y = y/H), transforming physical distances into dimensionless spatial variables. Velocity components are scaled relative to the reference inlet velocity (U = u/u_{in}, V = v/u_{in}), producing dimensionless velocity ratios that characterize flow magnitude. Pressure is expressed in terms of dynamic pressure (P = p/(ρu^2_{in})), where the denominator represents the kinetic energy per unit volume of the incoming flow. The thermal variable θ provides a normalized temperature measure by referencing the local temperature difference from inlet conditions (T- T_{in}) against the maximum potential temperature difference (T_w - T_{in}) between wall and inlet.

The variables and are the velocity components in the,) directions, pressure and temperature, respectively. Based on the dimensionless variables above, the dimensionless equations for the conservation of mass, momentum and thermal energy expressed as follows [26] [27]:

This system of equations governs steady state, two-dimensional, laminar flow and heat transfer of an incompressible fluid in a channel, including boundary transpiration effects such as fluid injection. The continuity equation (first equation) ensures mass conservation, maintaining incompressibility. The momentum equations (second and third)balance inertial forces, pressure gradients, and viscous dissipation, where viscosity is scaled by the geometric factor 2w/H and the inverse Reynolds number(Re)reflecting the ratio of inertial to viscous forces. The energy equation (fourth)combines convective heat transfer with conductive diffusion, that governed by the product of the Prandtl and Reynolds numbers (Pr Re), which relates momentum and thermal diffusivity. The 2w/H coefficient stands for wall transpiration, which models uniform fluid exchange at the boundaries and disturbs both velocity and temperature distributions. Put in dimensionless form, these equations allow scale-invariant analysis over different flow conditions, yet still capture the core physics of momentum and energy coupling in confined flows.

In the energy equation, viscous dissipation terms are dropped. The Reynolds number is defined as [expression], and the Prandtl number is defined as [expression]. The quantities α and v denote the thermal diffusivity and kinematic viscosity of the fluid, respectively. The Reynolds number is the ratio of inertial to viscous forces, whereas the Prandtl number is the ratio of momentum diffusivity to thermal diffusivity. The dimensionless form of the boundary conditions is presented in Table 1 as follows:

$$\frac{\partial U}{\partial X} + \frac{\partial V}{\partial Y} = 0$$
$$U\frac{\partial U}{\partial X} + V\frac{\partial U}{\partial Y} = -\frac{\partial P}{\partial X} + 2\frac{w}{H}\frac{1}{Re}\left(\frac{\partial^2 U}{\partial X^2} + \frac{\partial^2 U}{\partial Y^2}\right)$$
$$U\frac{\partial V}{\partial X} + V\frac{\partial V}{\partial Y} = -\frac{\partial P}{\partial Y} + 2\frac{w}{H}\frac{1}{Re}\left(\frac{\partial^2 V}{\partial X^2} + \frac{\partial^2 V}{\partial Y^2}\right)$$
$$U\frac{\partial \theta}{\partial X} + V\frac{\partial \theta}{\partial Y} = 2\frac{w}{H}\frac{1}{PrRe}\left(\frac{\partial^2 \theta}{\partial X^2} + \frac{\partial^2 \theta}{\partial Y^2}\right) \qquad (2)$$

Table 1. Boundary conditions for CFD computations [26] [30]

Boundary conditions	
Inlet port	$U = 1, V = 0, \theta = 0$
Four solid walls	$U = V = 0, \theta = 1$
Outlet port	U, V, θ are fully developed

With the outlet width fixed by W= 0.25, the velocity and temperature fields were also taken to be fully developed. From the foregoing

formulation, it is clear that the dimensionless parameters governing this problem are Re, Pr, S_o and W. In this study, the Prandtl number of the fluid was fixed at 5 for the validation model. The Reynolds number used was 100. The dimensionless pressure drop related to the difference between the average pressures of the inlet (Reference) and outlet ports with the flow kinetic energy by the following equation [26] [27]:

$$C_p = \frac{P - P_{ref}}{1/2\rho u_{in}^2} \quad (3)$$

The non-dimensional surface Nusselt number considered here to evaluate the local heat transfer in the walls by the following equation [26] [27]:

$$Nu_i = -\frac{\partial \theta}{\partial n}\Big|_{wall} \quad (4)$$

The thermal boundary conditions are defined such that all solid boundaries (bottom, left, right, and top walls) maintain a dimensionless temperature $\theta = 1$. In contrast, the incoming fluid exhibits $\theta = 0$ at the cavity entrance. The wall orientations are indexed by subscript i, with n denoting the outward normal vector for each boundary surface. The total Nusselt number gives the overall heat transfer contribution from all four thermally active walls, found by adding up the mean Nusselt numbers of each boundary surface [26] [27]:

$$\overline{Nu}_{tot} = \frac{1}{4}\sum_i \overline{Nu}_i = \frac{1}{4}\sum_i \frac{\int_{S_{i1}}^{S_{i2}} Nu_i dS}{(S_{i2} - S_{i1})} \quad (5)$$

To describe the heat transport ability of convective coolers, a dimensionless efficiency index ε is introduced based on wall, inlet, and outlet temperatures as:

$$\varepsilon = \frac{T_{wall} - T_{out}}{T_{wall} - T_{in}} \quad (6)$$

The ratio $\varepsilon = (T_{wall} - T_{out})/(T_{wall} - T_{in})$ works as a straightforward dimensionless indicator for evaluating how well a cooling system performs. The top part of the fraction $(T_{wall} - T_{out})$ tells us how much cooling was achieved, while the bottom part $(T_{wall} - T_{in})$ sets the upper limit of what is thermodynamically possible. At $\varepsilon = 0$, the outlet temperature matches the wall temperature, which means the coolant picked up no useful heat along the way. At $\varepsilon = 1$, the fluid reaches the inlet temperature upon leaving, a situation that corresponds to theoretically perfect cooling. The expression ties together all the ways heat moves through the system through solid walls, into the flowing fluid, and carried along by the flow itself by referencing the actual outcome against what the thermodynamics would allow at best. Given that ε always falls between 0 and 1, different systems can be put side by side regardless of their size, geometry, or the fluid used. From the early stages of design all the way through to real operating conditions, this coefficient remains a practical and informative measure. When ε goes up, the surface loses heat to the coolant more easily something that has made this parameter a familiar tool among engineers working on thermal management challenges.

The mixed fluid–ethylene glycol flow is injected as a new material from the configuration, under the same mathematical and geometrical conditions illustrated in Figure 1. The thermophysical parameters of this fluid mixture are constant, based on experimental results for the ethylene glycol (EG)-to-fluid ratios (0%, 25%, 50%, 75%, and 100%) reported in the literature [31] [32] and shown in Table 2. For the mathematical resolution of these energetic phenomena, a finite volume numerical method is employed via commercial code Ansys Fluent v17 to resolve the Navier-Stokes equations using Patankar's SIMPLE algorithm for pressure-velocity coupling [34]. The Least Squares Cell-Based method was used here to discretize the convection and diffusion terms in the flow conservation equations.

Additionally, the PRESTO scheme was adopted for the pressure equation, while the QUICK scheme was used to discretize the momentum and energy equations. The tolerance for the normalized residuals upon convergence criteria is set to 10^{-6} for all residual equations. The under-relaxation parameters for u, v, and T are set to 0.6 while the under-relaxation parameter for pressure correction is set to 0.3. The recipes and boundary interpolation at this resolution were gathered using hybrid initialization, as shown in Table 3.

Table 2. Thermo-physical properties of the base fluid and premixed fluids

Fluids	Thermo-physical properties [31] [32]			
	Density (Kg/m^3)	Specific heat (J/ Kg K)	Thermal conductivity (W/ m K)	Viscosity (Kg/ m s)
Purely Water	994	4183	0.6107	0.0007196
Water/EG (25%)	1026	3916	0.491504	0.00125639
Water/EG (50%)	1056	3516	0.3779673	0.002360452
Water/EG (75%)	1085	3030	0.3185966	0.004892834
Purely EG	1100	2454	0.248932	0.01138632

Table 3. Processing of CFD Ansys Fluent Parameters

Parameters	
Solution methods	
Scheme	Simple
Spatial discretization	
Pressure	PRESTO
Momentum	QUICK
Energy	QUICK
Solution controls	
Under-Relaxation Factors	
Pressure	0.3
Momentum	0.6
Energy	0.6
Convergence Criteria	10^{-6}
Solution Initialization	
Initialization Methods	Hybrid Initialization

3. Numerical validation

The present numerical study builds upon previous work [26], employing a uniform quadratic mesh (Shown in Figure 2) to achieve optimal geometry alignment and flow resolution. This grid configuration provides accurate gradient computation, particularly for temperature fields following x-axis and y-axis ($\partial T/\partial x$, $\partial T/\partial y$), while minimizing numerical diffusion in advection terms a critical factor for convective cooling analysis. Quadratic cells enhance numerical stability and convergence rates in simulations using the finite volume method (FVM), especially when handling smooth temperature gradients. Same-sized cells basically stop the solver from running into the kind of headaches that come up when cell shapes start varying across the mesh. A grid independence study was conducted (Figure 3 a-b) evaluating four mesh resolutions: $80^x \times 80^y$, $120^x \times 120^y$, $160^x \times 160^y$ and $200^x \times 200^y$ cells.

The analysis examined both pressure coefficient (C_p) and surface heat transfer coefficient at Re = 100, with width (W_o) = 0.25 and outlet port position $S_o = 1 + 2W_o$. As shown in Figure 3a–b, the solution demonstrates clear convergence as the grid is refined, with diminishing variability between successive mesh sizes, confirming that grid independence has been achieved. The same grid size of $160^x \times 160^y$ cells used in the literature [26], is selected after testing as it provides optimal numerical accuracy.

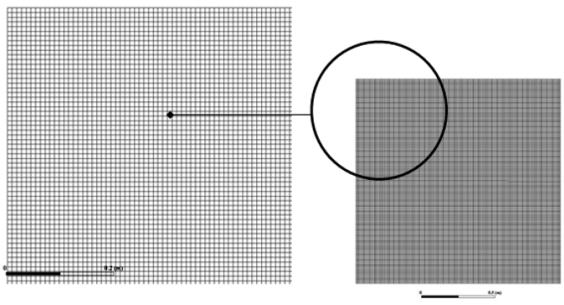

Figure 2. Grid mesh used of quadratic cell size

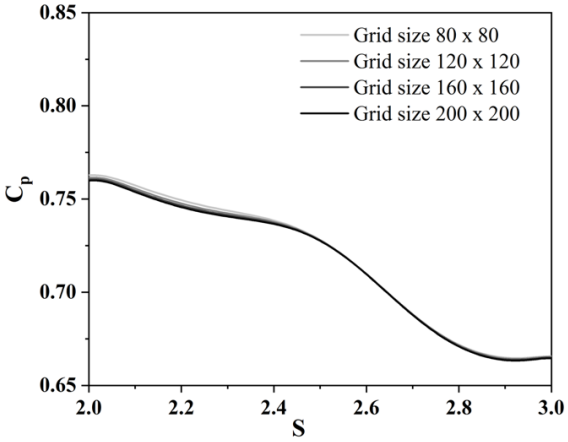

Figure 3. Grid mesh independency study for pressure coefficient **(a)** and surface heat transfer coefficient **(b)**

To validate the numerical code against experimental benchmarks, the study utilized data from Krane and Jessee [35] for a two-dimensional air-filled enclosure. Figure 4 illustrates the dimensionless temperature profiles along the vertical mid-plane of the cavity at a Rayleigh number (Ra) of 10^5. The numerical results, generated using a uniformly structured $160^x \times 160^y$ grid, that exhibit excellent alignment with both the experimental measurements of Krane and Jessee [35] and the computational findings of the numerical investigations [30] [36]. The same experimental validation way used by the literature [30] against Krane and Jessee [35] to aim develop the two-dimensional (2D) study of Saeidi et al. [26] into three dimensional (3D) physical model. This strong correlation reinforces the reliability of the adopted numerical approach for modeling convective heat transfer phenomena. For further validation in ventilated systems, the study referenced the laminar flow predictions of Saeidi et al. [26] within a two-dimensional (2D) enclosure. Both qualitative (Using ANSYS CFD-Post v17) and quantitative validations were performed by comparing results with those of Saeidi et al. [26] across various Reynolds numbers (Re) as presented in the comparison Table 4. Key

performance metrics including the pressure coefficient (Cp) and total Nusselt number (Nu_{tot}) are shown in Figure 5 a-b respectively and the qualitative comparison are displayed in the Figures 6-8. Based on these rigorous validations, the numerical methodology employed in this study is confirmed to deliver highly precise predictions of velocity fields, temperature distributions, Nusselt numbers, and cooling efficiency for the analyzed parameters.

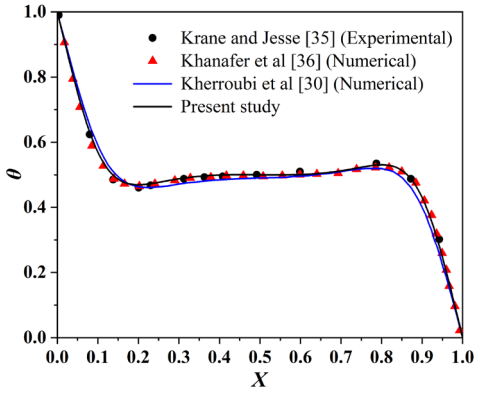

Figure 4. Comparative study of the temperature distribution with references [30], [35] and [36] for Ra = 1.89×10^5 and Pr = 0.71

Table 4. Total Nusselt number and pressure drop versus Reynolds number

Re	Saeidi et al [26]		Present work		Δ(%)	
	$\overline{Nu}_{tot}$	C_p	$\overline{Nu}_{tot}$	C_p	$\overline{Nu}_{tot}$	C_p
10	4.3600	7.5700	4.7458	7.0401	8.84	7
40	6.9342	2.6500	7.9336	2.5334	14.41	4.4
100	9.8485	1.7200	11.5027	1.6858	16.79	1.98
500	19.9028	1.4200	19.9473	1.3715	0.22	3.41

Δ(%): Computed discrepancy value between the present results and those of Saeidi et al. [26]

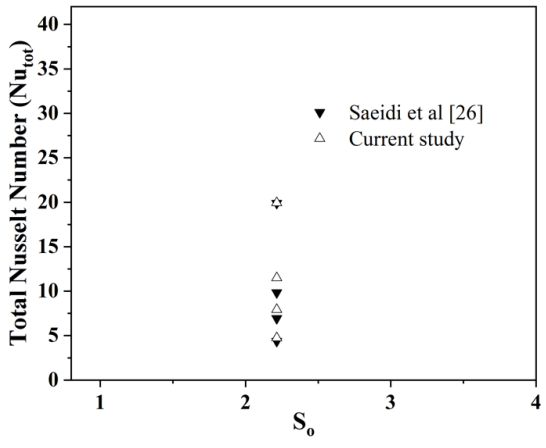

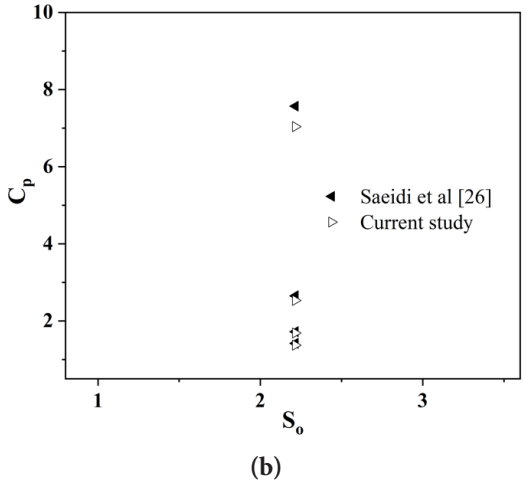

Figure 5. Quantitative validation for total Nusselt number (Nu_{to}) **(a)** and pressure coefficient **(b)**

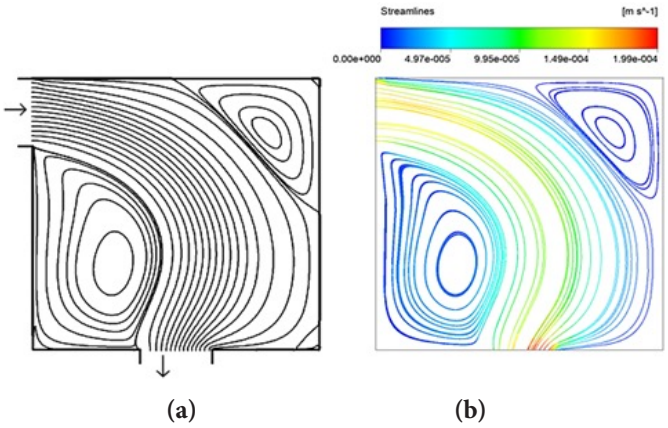

Figure 6. Validation of streamlines for Re = 100 of the literature [26] **(a)** and the present study **(b)**

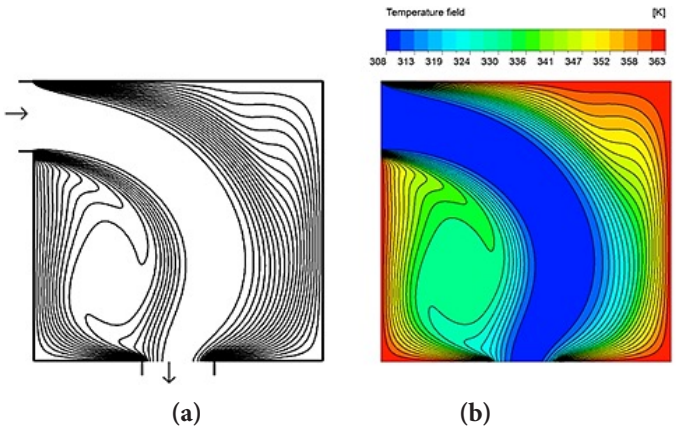

Figure 7. Validation of temperature field for Re = 100 of the literature [26] (a) and the current study (b)

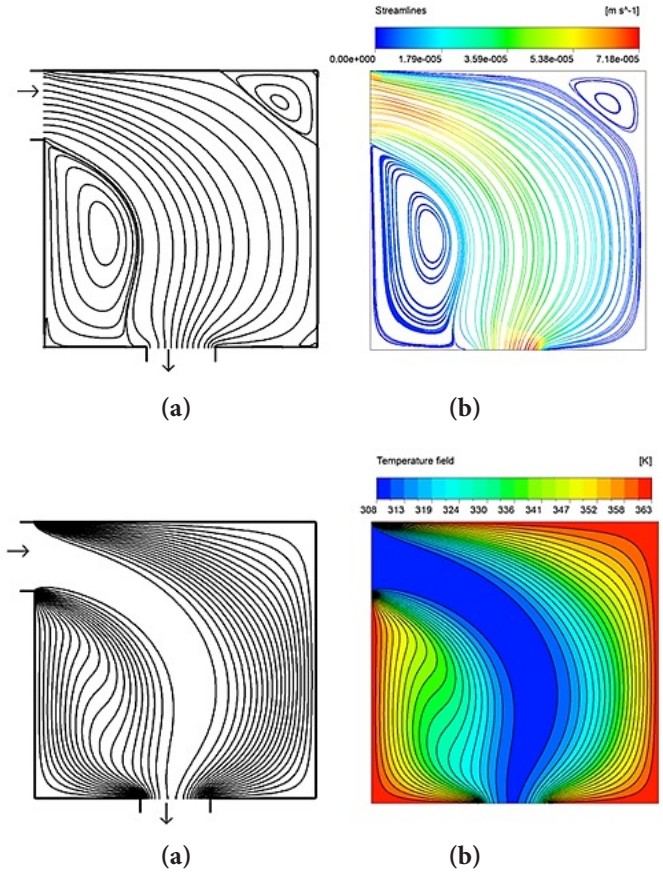

Figure 8. Qualitative Validation of both streamlines and temperature field for Re = 40 of the literature [26] **(a)** and the present study **(b)**

4. Results and discussions

The principal goal of this simulation is to evaluate the forced convection mechanism inside a square cavity surrounded by isothermal sources, under the viscous and body forces acting on the fluid-ethylene mixture flow. Mixtures with ethylene glycol (EG)-to-fluid ratios (0% (pure fluid), 25%, 50%, 75%, and 100% (pure ethylene glycol)) are injected downward at a constant Reynolds number, Re = 100. This Reynolds value is chosen for the low laminar regime to estimate the impact of the mixture fluid ratios on the dominance of fully forced convection at the outlet location of 2 + 0.5 W, which is identified as the optimal outlet position in the studied configuration [26]. The use of the ethylene glycol as an additive fluid is a common technic to enhance the thermal properties of HTF fluids exhibit good homogeneity and chemical stability in engine coolant fluid mixtures [33][37]. In addition to the mathematical formulations that describe the thermo-physical characteristics of the mixed ethylene glycol/fluid, real ratios (%) of ethylene glycol/fluid are derived from experimental data [31] to ensure that the fluid mixture doses impact the flow's thermo-fluidic behavior inside the square open system during the cooling process.

The aim of adopting a mixture of fluid/ethylene flow is to enhance the heat exchange process solely through forced convection during the cooling circulation of surrounded square cavity by isothermal heat source as discussed in the literature [26]. This involves the forced injection of pure fluid HTF and of premixed fluid/ethylene HTF at varying doses. The addition of 25-100% ethylene glycol to the base fluid significantly alters the thermo-physical properties of the mixture HTF as indicated in the experimental research [31]. A mixture with better thermophysical properties simply moves heat around faster during cooling, and diffusion works its way through the fluid going both ways. When more ethylene glycol is added, convective heat transfer picks up noticeably, driven by how density shifts across the fluid mixture once forced convection kicks in, as seen in the temperature-field plots of Figure 9. As the ethylene glycol share in the HTF mixture rises from 25% to 100%, the temperature inside the container shows a steady downward trend. This shift makes the mixture behave in a more diffusive manner, letting it pick up heat from the four isothermal walls and carry it toward the outlet more quickly, helped along by rising velocity, body forces, and viscous forces even as thermal conductivity goes down.

Pushing the ethylene glycol concentration from 25% to 100% stretches the forced-convection effect over a wider area inside the container, something that comes through clearly in the temperature field of Figure 9. At this stage, the HTF mixture flow takes over the thermal behavior of the container, which stands out especially in the temperature profile near the 298 K zone. This cooled region grows larger as more ethylene glycol is added to the mixture, as the temperature contours confirm. Body forces play a meaningful role here, steering the absorbed heat through a steady, well-coordinated interaction within the mixed-convection process. The density increases with increasing ethylene glycol concentration from 25% to 100%. In this case, rapid and substantial heat absorption by the high-density circulating mixture HTF increases the dominance of forced convection, driven by rapid body-force interactions between hot and cold mixture HTF particles. The flow velocity increases directly with ethylene glycol concentration from 25% to 100%, as shown by the streamline circulation patterns of pure ethylene glycol (100%) in Figure 11.

In the streamline visualization, two observed rotating vortices in the top-right and bottom-left corners of the cavity, as noted in the same numerical inquiry [26][30]. Most cases at different ethylene glycol rates (%) exhibit similar vortex patterns. The smaller top-right vortex rotates in a counterclockwise (CCW) direction, while the other larger one moves in a clockwise (CW) orientation as clarified in the vector velocity of the pure HTF fluid in Figure 10 as mentioned also in the literature [30], where the same numerical predictions for temperature field and streamlines have observed for purely water injection. The observed counterclockwise (CCW) and clockwise (CW) vortices in the top-right and bottom-left regions of the cavity (Figure 10), respectively, arise from synergistic interactions between forced convection and geometric constraints. The fluid flow introduced horizontally from the left inlet forms a high-velocity jet that

collides with the upper wall, inducing shear-layer separation at the top-right corner. This separation establishes a weaker CCW vortex via momentum-driven recirculation, while adverse pressure gradients near the bottom-left corner promote flow reversal and generate a dominant CW vortex as a secondary recirculation zone. The difference in vortex strength comes down to how the CCW vortex lines up with the main flow direction, while the CW vortex keeps going thanks to backflow that builds up because of where the inlet and outlet ports sit.

Changing the EG concentration anywhere between 25% and 100% tends to strengthen these flow structures, as higher viscosity shifts the viscous-inertial balance and helps vortices hold together, while the added density pushes momentum diffusion further and tightens spatial coherence. These results are broadly in line with what earlier pure-fluid studies found, though EG mixtures bring something different to the table by altering the way vortices and thermal behavior interact. Acting somewhat like heat reservoirs, the vortices trap warm fluid close to the walls and give convective heat transfer a boost, which shows up as higher Nusselt numbers in Figure 12. Consequently, the CW/CCW vortex pair is an inherent hydrodynamic feature of this geometry, driven by shear-layer instabilities and optimized by the thermo-physical properties of EG to enhance cooling efficacy.

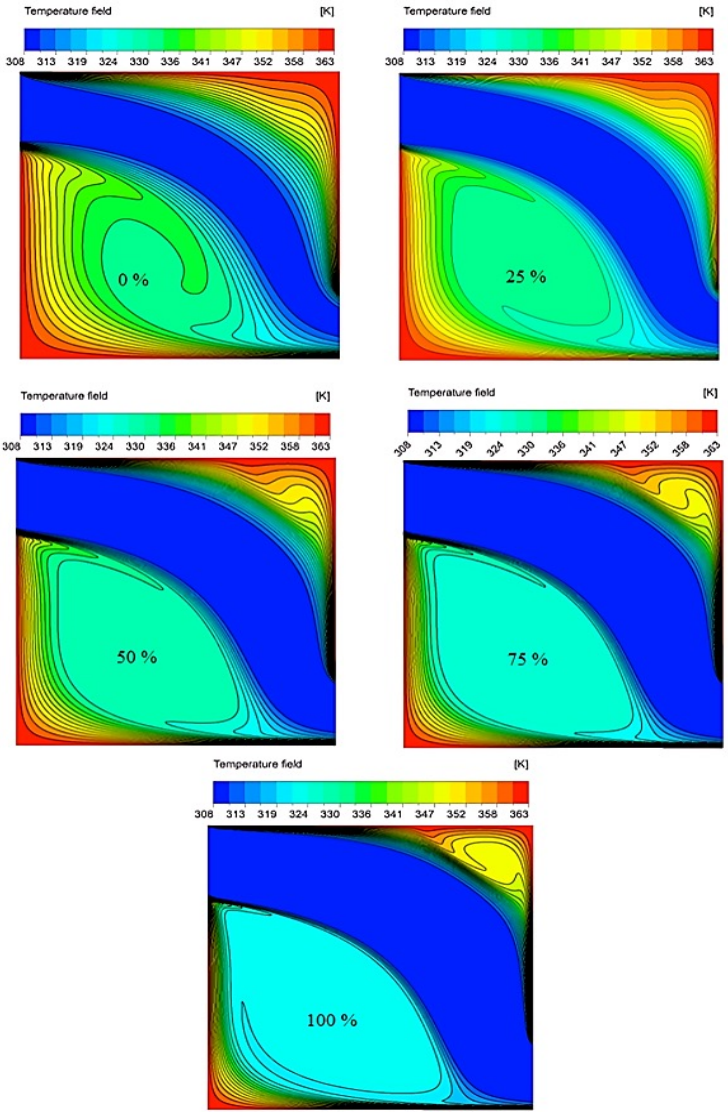

Figure 9. Temperature field for different ethylene glycol doses (25-100%)

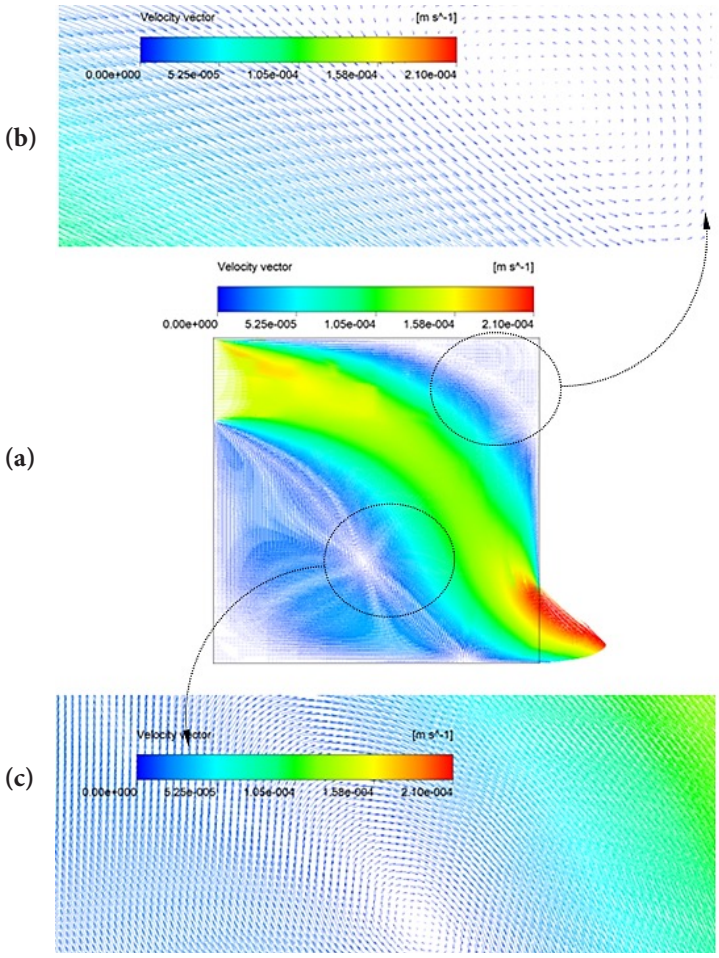

Figure 10. Normal **(a)** and enlarged **(b, c)** vector velocity views of pure fluid HTF

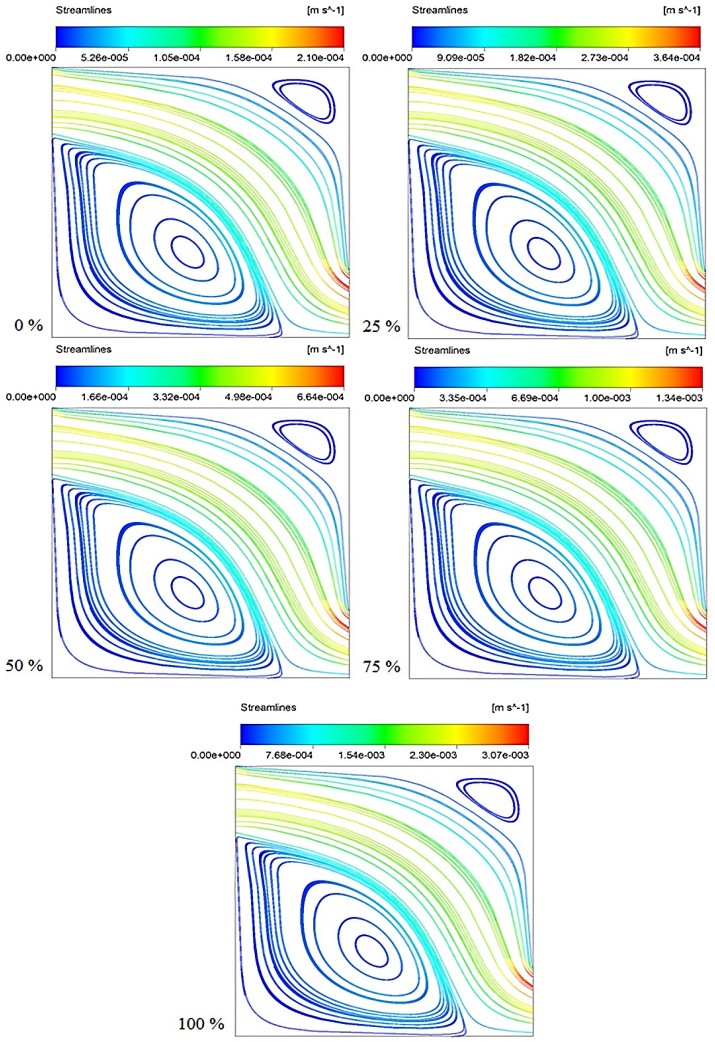

Figure 11. Streamlines visualization for different ethylene glycol doses (25-100%)

Despite the presence of rotating vortices, the mixed-fluid flow with varying ethylene glycol concentrations (%) exhibits velocity profiles, as illustrated in Figure 11. The 25% ethylene glycol mixture exhibits a higher non-rotational flow velocity of 3.64×10^{-4} m/s, compared with the pure heat transfer fluid (HTF) without ethylene glycol, which reaches 2.1×10^{-4} m/s. At the 25% concentration, the increasing dynamic viscosity enhances viscous forces, strengthening the boundary layers within the fluid flow, regarding to the comparison at fixed Reynolds number 100 that allows increasing the mixture H_2O/EG when the EF doses rise from 25 % to 100%. This effect, when combined with frictional interactions between rotating vortices and non-rotational flow regions, enhances the efficiency of forward fluid motion. Pure ethylene glycol HTF represents the optimal case for both cooling performance and fluid kinematic behavior, achieving a maximum streamline velocity of 3.07×10^{-3} m/s, which helps dominate forced convective cooling.

The surface Nusselt number is the preferred dimensionless variable for describing convective heat transfer relative to conductive heat transfer in this case. The evaluation of the surface Nusselt number is performed on four walls over the linear distance intervals S: [0.25-1], [1-2], [2.25-3], and [3-4], for ethylene glycol addition doses of 25-100% during the cooling process. The pure HTF, which does not contain ethylene glycol, exhibits the lowest average surface Nusselt number over time compared with the other cases. The addition of 25-100% ethylene glycol to the fluid mixture increases the contact resistivity between the fluid mixture and the surrounding walls, due to increases in velocity and density. This physical behavior enhances heat convection, particularly in the distance intervals S [1-2] and [3-4], as a result of the alignment of the flow direction with the wall positions as shown in Figure 12.

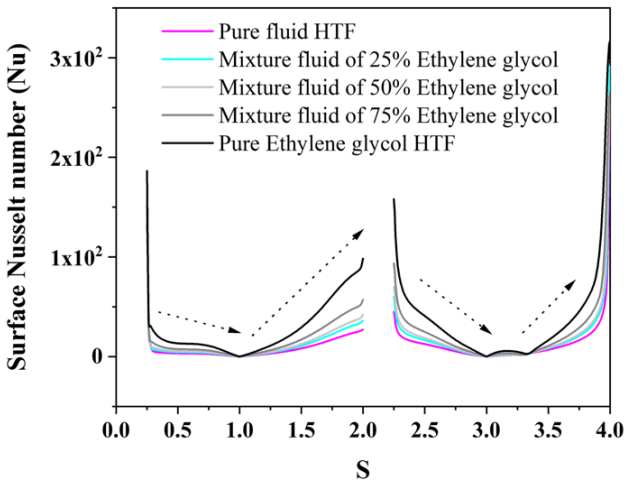

Figure 12. Surface Nusselt number evaluation for different distance along the walls S

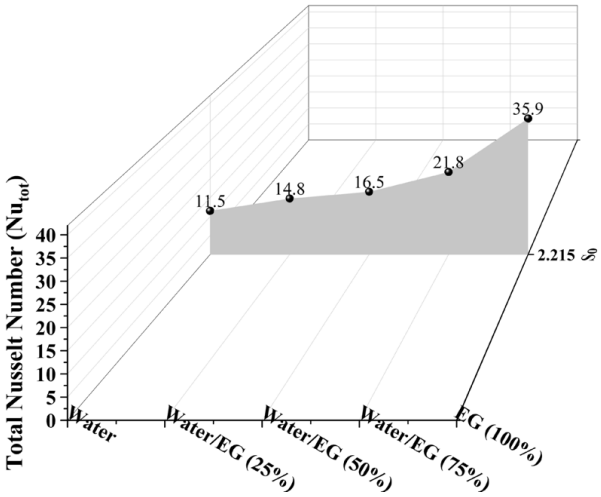

Figure 13. Total Nusselt number (Nu $_{tot}$) evolution at different ethylene glycol doses (%)

This study investigates the effect of different fluid compositions on convective heat-transfer efficiency inside a square cavity subjected to a thermal gradient. The total Nusselt number (Nu $_{tot}$) that shown in the Figure 13 are measured for different doses mixtures of water and ethylene glycol, revealing significant variations that underscore the importance of fluid selection in thermal management applications. Figure 13 illustrates a progressive increase in the total Nusselt number with increasing concentrations of ethylene glycol. For pure water, the Nusselt number is 11.5, suggesting relatively low convective heat-transfer efficiency compared with the more viscous mixtures. The addition of 25 % from the ethylene glycol allows increasing the total Nusselt number (Nu $_{tot}$) to 14.8 that indicates the addition of ethylene glycol enhances thermal conductivity and reduces viscosity, and facilitating more efficient heat transfer regime. The further increase to 16.5 is consistent with enhanced convective currents and improved thermal diffusion properties, owing to the unique thermal characteristics of the 50% ethylene glycol mixture. A Nusselt number of 21.8 at 75% ethylene glycol tells you the fluid is getting pretty close to peak convective behavior, with heat transport picking up noticeably at that point. Hitting a peak value of 35.9, pure ethylene glycol turns out to deliver the highest convective heat transfer efficiency among the tested fluids. This comes down to its thermal characteristics, particularly a higher specific heat capacity and a lower viscosity relative to water. Ethylene glycol carries higher density and dynamic viscosity, yet still maintains acceptable thermal conductivity, which helps push heat transfer rates up as concentration grows at a fixed Reynolds number of 100 a quality that matters a lot wherever fast cooling is needed.

This work looks at how well different fluid mixtures perform thermally inside a square cavity cooling setup, with the inlet held at 35°C and the walls kept at 90°C. Heat transfer efficiency was tracked across a range of ethylene glycol concentrations in water, and the differences observed point clearly to how much fluid properties can shape cooling behavior.

Figure 14 lays out the cooling efficiency (ε) for each fluid tested. With each increase in ethylene glycol content, efficiency moves higher, kicking off at 87.4% for plain water and topping out at 98.3% for pure ethylene glycol. The fluid composition clearly has a strong hand in how well heat gets handled during convective cooling. Plain water, as the starting reference, came in at 87.4%, where its own viscosity and thermal conductivity under the test conditions kept it from going higher. Once 25% ethylene glycol was brought in, a noticeable jump to 92% followed. Viscosity came down and thermal conductivity went up, and between the two, the fluid had an easier time moving through the system and giving off heat. At 50%, the reading climbed to 95.2%, with the mixture still fluid enough to circulate well while pulling more out of its thermal characteristics. At 75%, the mixture was already brushing up against its best possible output, making good use of ethylene glycol's thermal side while keeping viscosity from climbing too high. Pure ethylene glycol at 100% wrapped things up at 98.3%, and it is not hard to see why its properties just lend themselves naturally to taking in and moving heat, which makes it a solid pick for cooling jobs where performance really matters. The fact that efficiency kept rising with each step up in concentration comes down to how thermal conductivity, viscosity, and specific heat capacity all move in the right direction as ethylene glycol gradually takes over from water in the mixture.

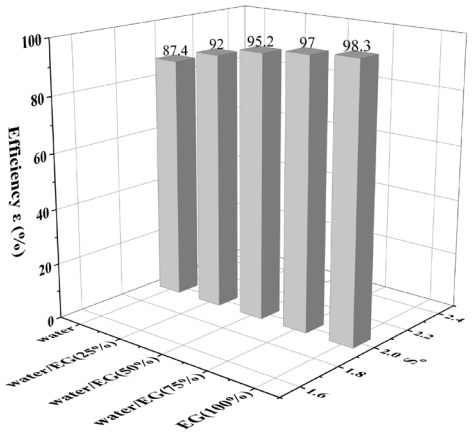

Figure 14. Efficiency of cooling process for different ethylene glycol doses (%)

5. Conclusion

A finite-volume numerical method, based on the Navier-Stokes equations for laminar flow, was applied to solve the two-dimensional (2D) cooling process in a square container representative of electrical/electronic cabins. The study examines mixtures of water with ethylene glycol concentrations ranging from 25% to 100%, injected luminary into an isothermal cavity following the geometric configuration of the reference [26]. This setup allows the evaluation of the effects of physical parameters on forced-convection heat transfer under steady-state conditions. The main results of this numerical inquiry are:

- Increasing the ethylene glycol concentration causes bidirectional changes in velocity by altering fluid density and viscosity. Near the walls and boundary layers, forced convection gets a stronger push from this effect. Plain water tops out at a maximum velocity of 2.10×10^{-4} m/s, while mixtures carrying 25%, 50%, 75%, and 100% ethylene glycol go noticeably higher, hitting 3.64×10^{-4} m/s, 6.64×10^{-4} m/s, 1.34×10^{-3} m/s, and 3.07×10^{-3} m/s in that order. As the fluid moves faster, the flow becomes more active and heat exchange within the corner rotational vortices picks up as well.
- Addition of ethylene glycol (25-100%) increases the dominance of forced convection over conductive heat transfer, as evidenced by the evolution of the Nusselt number. This modifies the thermal and hydrodynamic behavior of the fluid mixture that directly influencing the total Nusselt number (Nu_{tot}), and effect on fluid velocity and vortex dynamics (as observed in the results study)that can increase the total Nusselt number in forced convection systems from 11.5 to 14.8, 16.5, 21.8 and 35.9 during the addition of doses 25%, 50%, 75% and 100% respectively
- At optimal ethylene glycol concentrations (25–100%), enhanced fluid circulation significantly improves heat redistribution efficiency relative to pure water. This improvement persists even with EG's reduced specific heat capacity, demonstrating that in confined cavity systems the advantages of altered convective flow regimes outweigh thermal conductivity limitations. Consequently, cooling performance increased sequentially from 87.4% to 92%, 95.2%, 97%, and 98.3% with the addition of 25%, 50%, 75%, and 100% doses, respectively. These results confirm that EG-water blends can achieve superior cooling capabilities in thermal management systems where precise flow control governs performance.

Future work will involve developing new 3D geometries and physical parameters high Reynolds (Re) numbers.

References

[1] Ullah, A., Kilic, M., Habib, G., Sahin, M., Khalid, R. Z., & Sanaullah, K. Reliable prediction of thermophysical properties of nanofluids for enhanced heat transfer in process industry: A perspective on bridging the gap between experiments, CFD and machine learning. Journal of Thermal Analysis and Calorimetry;2023. 148(12),5859–5881. https://doi.org/10.1007/s10973-023-12083-7

[2] Kilic, M., Sahin, M., & Abdulvahitoglu, A. A new approach for enhancing the effectiveness of a regenerative heat exchanger by using organic and inorganic phase change material. Journal of Thermal Analysis and Calorimetry; 2024. 149(22), 13081–13093. https://doi.org/10.1007/s10973-024-13599-2

[3] Dal, A., Şahin, M., & Kılıç, M. A thermohydrodynamic performance analysis of a fluid film bearing considering geometrical parameters. Journal of Thermal Engineering; 2023. 9(6), 1604–1617. https://doi.org/10.18186/thermal.1401279

[4] Wang Q, Li J, Ren Y, Li J, Li J, Ma M. Comparison study of natural convection between rectangular and triangular enclosures. AIP Adv 2021;11(4). https://doi.org/10.1063/5.0035007

[5] Rani, H.P., Narayana, V., Jayakumar, K.V. Geometrical Effects on Natural Convection in 2D Cavity. In: Dutta, D., Mahanty, B.(eds)Numerical Optimization in Engineering and Sciences. Advances in Intelligent Systems and Computing, vol 979. Springer, Singapore; 2020. https://doi.org/10.1007/978-981-15-3215-3_37

[6] Triveni MK, Panua R. Numerical analysis of natural convection in a triangular cavity with different configurations of hot wall. Int J Heat Technol 2017;35(1):11-18. https://doi.org/10.18280/ijht.350102

[7] Saleem KB, Alshara AK. Natural convection in a triangular cavity filled with air under the effect of external air stream cooling. Heat Transf-Asian Res 2019;48(7):3186-3213. https://doi.org/10.1002/htj.21537

[8] Nogueira RM, Martins MA, Ampessan F. Natural convection in rectangular cavities with different aspect ratios. Rev Eng Térmica 2011;10(1–2):44. https://doi.org/10.5380/reterm.v10i1-2.61951

[9] Phu NM, Hap NV. Numerical investigation of natural convection and entropy generation of water near density inversion in a cavity having circular and elliptical body. Comput Overview Fluid Struct Interact 2020;121. https://doi.org/10.5772/intechopen.95301

[10] Cesini G, Paroncini M, Cortella G, Manzan M. Natural convection from a horizontal cylinder in a rectangular cavity. Int J Heat Mass Transf 1999;42(10):1801-1811. https://doi.org/10.1016/S0017-9310(98)00266-X

[11] Ha MY, Jung MJ. A numerical study on three-dimensional conjugate heat transfer of natural convection and conduction in a differentially heated cubic enclosure with a heat-generating cubic conducting body. Int J Heat Mass Transf 2000;43(23):4229-4248. https://doi.org/10.1016/S0017-9310(00)00063-6

[12] Park YG, Ha MY, Yoon HS. Study on natural convection in a cold square enclosure with a pair of hot horizontal cylinders positioned at different vertical locations. Int J Heat Mass Transf 2013; 65:696-712. https://doi.org/10.1016/j.ijheatmasstransfer.2013.06.059

[13] Chandra Pal G, Goswami N, Pati S. Numerical investigation of unsteady natural convection heat transfer and entropy generation from a pair of cylinders in a porous enclosure. Numer Heat Transf Part A: Appl 2018;74(6):1323-1341. https://doi.org/10.1080/10407782.2018.1507887

[14] Adjlout L, Imine O, Azzi A, Belkadi M. Laminar natural convection in an inclined cavity with a wavy wall. Int J Heat Mass Transf 2002;45(10):2141-2152. https://doi.org/10.1016/S0017-9310(01)00304-0

[15] Mushate KS. CFD prediction of natural convection in a wavy cavity filled with porous medium. Glob J Res Eng 2011; 11:29-45.

[16] Horimek, Abderrahmane, and El-Amria Nekag. "Natural Convection Cooling of a Heat Source Placed at the Bottom of a Square Cavity. Effect of Source Length, Position, Thermal Condition and Prandtl Number." International Journal of Heat & Technology 38, no. 3(2020).https://doi.org/10.18280/ijht.380317

[17] Aminossadati, S. M., and B. Ghasemi. "Natural convection cooling of a localised heat source at the bottom of a nanofluid-filled enclosure." European Journal of Mechanics-B/Fluids 28, no. 5 (2009): 630-640. https://doi.org/10.1016/j.euromechflu.2009.05.006

[18] El Hattab, Mohamed, Mustapha Boumhaout, and Soufiane Oukach. "MHD natural convection in a square enclosure using carbon nanotubewater nanofluid with two isothermal fins." Sigma Journal of Engineering and Natural Sciences 42, no. 4 (2024): 1075-1087. https://doi.org/10.14744/sigma.2024.00089

[19] Shahi, Mina, Amir Houshang Mahmoudi, and Farhad Talebi. "Numerical study of mixed convective cooling in a square cavity ventilated and partially heated from the below utilizing nanofluid." International Communications in Heat and Mass Transfer 37, no. 2 (2010): 201-213. https://doi.org/10.1016/j.icheatmasstransfer.2009.10.002

[20] Sereır, T., Mıssoum, A., Mebarkı, B., Elmır, M., et al. Effect of the position of the hot source on mixed convection in a rectangular cavity. Journal of Thermal Engineering; 2022. 8(4),538-550. https://doi.org/10.18186/thermal.1150294

[21] Mahmoudi A, Mejri I, Omri A. Study of natural convection in a square cavity filled with nanofluid and subjected to a magnetic field. Int J Heat Technol 2016;34(1):73-79. https://doi.org/10.18280/ijht.340111

[22] Bhuiyana AH, Alam MS, Alim MA. Natural convection of water-based nanofluids in a square cavity with partially heated bottom wall. Procedia Eng 2017; 194:435-441. https://doi.org/10.1016/j.proeng.2017.08.168

[23] Boulahia Z, Wakif A, Chamkha AJ, Sehaqui R. Numerical study of natural and mixed convection in a square cavity filled by a Cu–water nanofluid with circular heating and cooling cylinders. Mech Ind 2017;18(5):502. https://doi.org/10.1051/meca/2017021

[24] Boulahia Z, Wakif A, Sehaqui R. Numerical modeling of natural convection heat transfer in a wavy wall enclosure filled by a Cu-water nanofluid with a square cooler. J Nanofluids 2017;6(2):324-333. https://doi.org/10.1166/jon.2017.1315

[25] Rahmati AR, Tahery AA. Numerical study of nanofluid natural convection in a square cavity with a hot obstacle using lattice Boltzmann method. Alex Eng J 2018;57(3):1271-1286. https://doi.org/10.1016/j.aej.2017.03.030

[26] Saeidi SM, Khodadadi JM. Forced convection in a square cavity with inlet and outlet ports. Int J Heat Mass Transf 2006;49(11-12):1896-1906. https://doi.org/10.1016/j.ijheatmasstransfer.2005.10.033

[27] Saeidi, S. M. Fluid flow and heat transfer in cavities with inlet and outlet ports: Effect of flow oscillation and application to design of microvalves (Doctoral dissertation, Auburn University). 2005. Auburn University Theses and Dissertations.

[28] Singh S, Sharif MAR. Mixed convective cooling of a rectangular cavity with inlet and exit openings on differentially heated side walls. Numer Heat Transf Part A: Appl 2003;44(3):233-253. http://dx.doi.org/10.1080/716100509

[29] Omri A, Ben Nasrallah S. Control volume finite element numerical simulation of mixed convection in an air-cooled cavity. Numer Heat Transf Part A: Appl 1999;36(6):615-637. http://dx.doi.org/10.1080/104077899274606

[30] Kherroubi, Seddik, et al. "Two-and three-dimensional comparative study of heat transfer and pressure drop characteristics of nanofluids flow through a ventilated cubic cavity (part I: Newtonian nanofluids)." Journal of Thermal Analysis and Calorimetry 2021;144: 623-646. https://doi.org/10.1007/s10973-020-09588-w

[31] Bohne D, Fischer S, Obermeier E. Thermal, conductivity, density, viscosity, and Prandtl-numbers of ethylene glycol-water mixtures. Ber Bunsenges Phys Chem 1984;88(8):739-742.2. https://doi.org/10.1002/bbpc.19840880813

[32] Dinçer, İ., and Calin Zamfirescu. "Appendix B thermophysical properties of Water." Drying Phenomena:Theory and Applications 2016; 457-459.
[33] Yue H, Zhao Y, Ma X, Gong J. Ethylene glycol: properties, synthesis, and applications. Chem Soc Rev 2012;41(11):4218-4244. https://doi.org/10.1039/C2CS15359A
[34] Patankar S. Numerical heat transfer and fluid flow. CRC Press; 2018. https://doi.org/10.1201/9781482234213
[35] Krane, R. Jessee. "Some detailed field measurements for a natural convection flow in a vertical square enclosure." In Proceedings of the First ASME-JSME Thermal Engineering Joint Conference, 1983, vol. 1, pp. 323-329.
[36] Khanafer, K., Vafai, K., & Lightstone, M. Buoyancy-driven heat transfer enhancement in a two-dimensional enclosure utilizing nanofluids. International Journal of Heat and Mass Transfer; 2003. 46(19),3639–3653. https://doi.org/10.1016/S0017-9310(03)00156-X
[37] Jack TK, Ojapah MM. Water-cooled petrol engines: a review of considerations in cooling systems calculations with variable coolant density and specific heat. Int J Adv Eng Technol 2013;6(2):659.